

The Irreversible Form II to Form I Transformation in Random Butene-1/Ethylene Copolymers

Maria Laura Di Lorenzo^{*1}, René Androsch², Maria Cristina Righetti³

¹ Consiglio Nazionale delle Ricerche, Istituto per i Polimeri, Compositi e Biomateriali – c/o
Comprensorio Olivetti – Via Campi Flegrei, 34 – 80078 Pozzuoli (NA) – Italy

² Martin-Luther-University Halle-Wittenberg, Center of Engineering Sciences, D-06099
Halle/Saale, Germany

³ Consiglio Nazionale delle Ricerche, Istituto per i Processi Chimico-Fisici, INSTM, UdR Pisa, Via
G. Moruzzi 1, 56124 Pisa, Italy

Abstract

The influence of both temperature and time on the solid-solid transformation from tetragonal Form II mesophase to trigonal Form I crystals in isotactic poly(butene-1) and its random copolymers with ethylene has been evaluated. The polymers were isothermally crystallized and then annealed at temperatures ranging from -30 to +30 °C for various times, up to 24 hours. Incorporation of ethylene co-units into isotactic poly(butene-1) not only leads to a faster solid-solid transformation rate, as already discussed in the literature, but it also affects the temperature of maximum transformation rate. For all the analyzed compositions, at the initial stage of the process, a maximum rate is observed upon annealing around -20 °C, whereas when the transition proceeds to a later stage, it becomes much faster around +20 °C. The occurrence of two maxima in the transformation-temperature profile has been correlated with a nucleation and growth mechanism for the Form II to Form I transition. The influence of ethylene co-units on the transformation rate has been rationalized taking into account the varied composition of the rigid amorphous portions at the lamellar basal planes of the crystals, which confirms the hypothesis of a connection between crystal lamellae rearrangements and the amorphous-crystal boundaries.

* Corresponding author email address: dilorenzo@ictp.cnr.it

Introduction

Isotactic poly(butene-1) (iPB-1) is a polymorphic polyolefin that displays three major crystal modifications, depending on the crystallization conditions.¹ From the melt, iPB-1 crystallizes in a tetragonal crystal lattice, named Form II, with $a = 1.542$ nm and $c = 2.105$ nm, where c is the chain axis.² Structure determination yielded an 11_3 conformation for helices with opposite chirality.^{2,3} Growth of Form II crystals is kinetically favored when iPB-1 is crystallized by cooling the unstrained melt at atmospheric pressure, and upon storage it spontaneously and irreversibly transforms into the twinned trigonal Form I. The transformation is completed after about 10 days at room temperature, and takes longer at higher or lower temperatures.¹

Form II has conformational disorder, due to molecular motions destroying the short-range order within the helix, which makes this modification a conformationally disordered (condis) crystal.⁴ At room temperature the methyl side group rotates about its axis, and this local motion is transmitted to the backbone of the chains within the crystalline domains.^{5,6}

In the Form I, iPB-1 chains adopt left-handed and right-handed 3_1 helix conformations, packed in a trigonal lattice with the unit cell parameters $a = 1.77$ nm and $c = 0.65$ nm.⁷ The third polymorph, Form III, is not obtained by melt processing, but only from solutions by evaporation of the solvent, therefore it has limited interest for industrial applications. Form III has helices of a single chirality with 4_1 symmetry, packed in an orthorhombic lattice⁸⁻¹² with $a = 1.238$ nm, $b = 0.888$ nm, and $c = 0.756$ nm.²

The polymorphic transformation from the tetragonal Form II condis modification to the trigonal Form I crystals involves remarkable variations of mechanical properties, including higher hardness, stiffness, and strength. Also the thermal properties are affected by the crystal transformation, as Form I crystals have a higher melting temperature and melting enthalpy than Form II.^{1,13-16} The transformation rate can be tailored by incorporation of random 1-alkene co-units in the butene-1 chain: in random copolymers of butene-1 with linear 1-alkenes containing more than 5 carbon atoms or branched co-units, the Form II to Form I transformation is retarded, while ethylene, propylene, or 1-pentene co-units accelerate the transformation from the condis mesophase to the trigonal crystals.³

Prior investigations revealed that ethylene co-units in random butene-1/ethylene copolymers are mostly excluded from crystallization.^{17,18} This affects the crystallization kinetics of the copolymers, as the rates of formation and growth of Form II spherulites decrease with increasing molar percentage of ethylene co-units in the butene-1 chain.^{3,19-21} The exclusion of ethylene co-units from crystallization in random butene-1/ethylene copolymers and their accumulation at the crystal basal planes affects the fold-surface structure of crystals of iPB-1, quantified by a distinct increase

in the fold-surface free energy, and also leads to a marked increase in the specific rigid amorphous fraction with increasing concentration of co-units.^{20,21} Conversely, inclusion of ethylene co-units into the butene-1 chains leads to an acceleration of the rate of the polymorphic transformation of the unstable Form II phase into stable trigonal Form I crystals.^{3,22} The latter was quantified by isothermal crystallization of the tetragonal crystals at 20 °C, followed by annealing at various temperatures, ranging from 0 to 60 °C. It was found that the presence of ethylene co-units highly enhances the transformation kinetics, and that the rate of the process strongly depends on the annealing temperature.^{3,22} A tentative explanation was proposed, based on the migration and redistribution of the defects initially trapped in the crystal lattice, as random copolymerization with ethylene co-units results in a composition-dependent partitioning of the defect content in the crystals.²² This mechanism is now reviewed, based on recent findings on the crystallization kinetics, structure and morphology of random butene-1/ethylene copolymers. Such findings proved only minor inclusion within the crystals of ethylene co-units, which mostly accumulate at the crystal fold-surface.^{17,20} This affects not only the crystallization kinetics, but also the three-phase composition, with a varied mobility of the amorphous chains which is determined not only by crystallization conditions, but also by the co-unit content.²¹

In order to shed light on the irreversible tetragonal to trigonal transformation, random butene-1/ethylene copolymers of different compositions were isothermally crystallized, then aged at various temperatures between the glass transition temperature and room temperature. A more thorough knowledge of the mechanism of this polymorphic transition is of enormous importance, due to its large impact on material properties. This will allow to further tailor the structure-property relations of iPB-1 homopolymer, whose commercial development has been limited by the poor understanding and control of the slow Form II to Form I transformation process,^{12,22-26} as well as of random butene-1/ethylene copolymers, which have a large economic importance, being used, e.g., as component in the seal layer of easy-opening packaging films.²⁷⁻²⁹

Experimental part

Random isotactic butene-1/ethylene copolymers were obtained from Lyondell Basell (Germany). Table 1 is a list of the homo- and copolymers used in this work, including information about the concentration of ethylene co-units and the mass-average molar mass.^{14,28} The as-received sample chips were processed to films of 500 µm thickness by compression-molding using a Perkin-Elmer FTIR press in combination with a Lot-Oriel/Specac film maker die and heating accessory.

Table 1. List of isotactic random butene-1/ethylene copolymers used in this work, including information about the content of ethylene co-units and the mass-average molar mass.

Trade name ²⁹	Ethylene content		Molar mass kg mol ⁻¹ ^{22,29}
	mol%	m% ²²	
PB 0300M	0	0	347
PB 8640M	1.5	0.75	470
PB 8220M	4.3	2.2	400

Thermal analysis was conducted with a Perkin-Elmer Pyris Diamond DSC, equipped with an Intracooler II as cooling system. The instrument was calibrated regarding temperature with high purity standards (indium and cyclohexane) and regarding energy by the heat of fusion of indium. Dry nitrogen was used as purge gas at a flow rate of 48 ml min⁻¹.

The isotactic butene-1 homopolymer and the random isotactic butene-1/ethylene copolymers were isothermally crystallized at a fixed temperature (T_c) for 25 min. Due to the largely different crystallization kinetics, it was not possible to select a single crystallization temperature for the three analyzed grades. It must be underlined that the scope of this study is not to compare and quantify the kinetics of transformation from Form II to Form I crystals as function of ethylene content, which is well detailed in the literature,^{11,17-22} but to provide new insights into the mechanism of this solid-solid phase transition.

After isothermal crystallization at T_c , the polymers were rapidly cooled at maximum rate to the annealing temperature (T_a) ranging from -30 to +30 °C, and there maintained for a time (t_a) ranging from 1 to 1440 min (24 hours). The thermal behavior after isothermal annealing was then analyzed by heating the samples from T_a to a temperature higher than the melting point at 100 K min⁻¹. A high heating rate was chosen in order to avoid or reduce as much as possible potential further solid-solid transition during heating.

The contribution to the whole melting process of the individual Form II and Form I melting peaks was determined from the DSC curves by means of the multiple peakfit program of the commercial software Origin Pro (OriginLab Corporation). In order to separate the two non-symmetric partially overlapping melting peaks, a non-linear curve fitting was performed by using the exponentially modified Gaussian function:¹⁴

$$f(T) = \frac{A}{\tau} \exp\left[\frac{1}{2}\left(\frac{w}{\tau}\right)^2 - \frac{T - T_c}{\tau}\right] \int_{-\infty}^z \frac{1}{\sqrt{2\pi}} \exp\left(-\frac{y^2}{2}\right) dy$$

with $z=[(T-T_c)/w-w/\tau]$, where A is the peak area, τ the peak distortion, w the peak width and T_c the position of the peak maximum. Some examples of the fit, collected in Figure 1, show that the exponentially modified Gaussian function describes satisfactorily the experimental curves in the melting region of both the homopolymer and the copolymers. The displayed examples also prove that a good fit can be obtained when each of the two endotherms are either small or large in size, as well as when their size is comparable. The fraction of Form I and Form II crystals, $X_{\text{cry(I)}}$ and $X_{\text{cry(II)}}$, was determined by comparison of the calculated peak areas with the bulk melting enthalpy of Form I and Form II crystals, which amount to 141 and 62 J g⁻¹, respectively.¹⁴

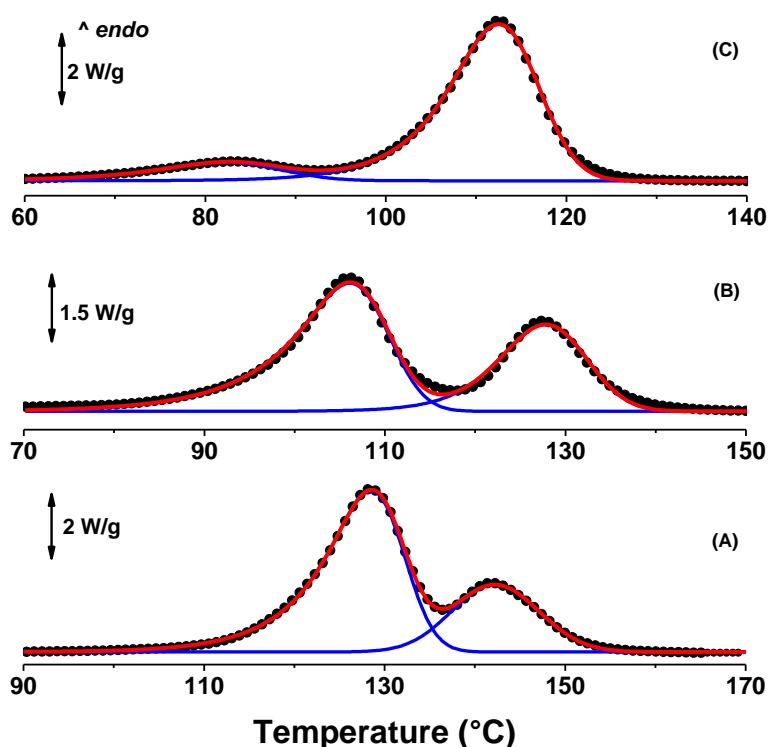


Figure 1. Examples of multiple peakfit analysis of the DSC curves in the melting region of (A) iPB-1 homopolymer, (B) butene-1/ethylene random copolymer containing 1.5 mol% of ethylene, and (C) butene-1/ethylene random copolymer containing 4.3 mol% of ethylene, after isothermal crystallization at the respective T_c for 25 min and annealing at $T_a = 0$ °C for 480 min. The fit was obtained by using the exponentially modified Gaussian function (close black circles: experimental curves; blue solid lines: resolved peaks; red solid lines: sum of the resolved peaks).

Results and Discussion

The thermal behavior of the iPB-1 homopolymer and of the random copolymers after isothermal crystallization at T_c for 25 min, followed by cooling to -70 °C, is illustrated in Figure 2. The major thermal events detected in Figure 2 include the glass transition of the mobile amorphous fraction (MAF) at a temperature $T_{g,MAF}$ of about -30°C, which shifts to lower temperatures with

increasing ethylene content,²⁰ and two endothermic peaks. The endotherm at lower temperature is due to melting of the Form II mesophase, and the peak at higher temperature is associated to melting of Form I crystals. In the copolymer with ethylene content of 4.3 mol%, multiple peaks appear, caused by melting of crystals with different thermal stability. Copolymerization of ethylene with butene-1 causes melting of both Form II and I modifications at lower temperatures, as discussed in Ref. 22. Moreover, a weak exothermic event appears in the c_p curves at temperatures slightly below 0 °C, indicated by the thick green arrow in Figure 2. To our knowledge, such exothermic peak has not been discussed in the literature and is the object of the thermal analysis discussed below.

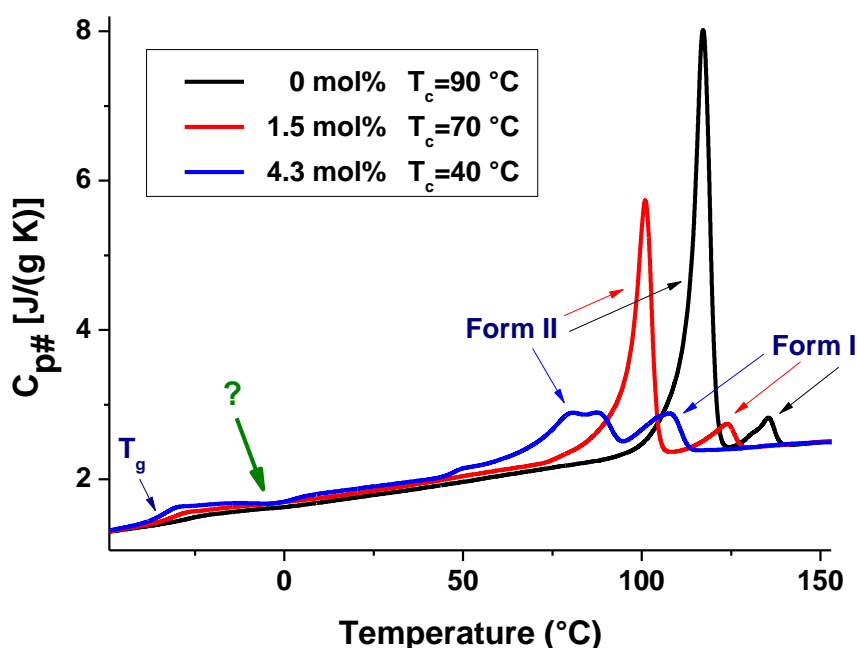


Figure 2. Apparent specific heat capacity ($c_{p\#}$) of isotactic poly(butene-1) and of butene-1/ethylene random copolymers containing 1.5 and 4.3 mol% of ethylene, isothermally crystallized at the indicated temperatures, cooled to -70 °C, and then heated at 100 K min⁻¹. Thermal events occurring during heating are indicated by arrows.

The three analyzed iPB-1 based polymers were isothermally crystallized at the indicated temperatures for 25 min, leading to different values of the crystal fraction (X_{cry}), mobile amorphous fraction (MAF), rigid amorphous fraction (RAF), and specific RAF ($RAF_{sp}=RAF/X_{cry}$). The crystal fraction was obtained from the enthalpy of isothermal crystallization, the mobile amorphous fraction was quantified by the heat-capacity increment at the glass transition temperature, and the rigid amorphous fraction was determined by the difference $RAF = 1 - X_{cry} - MAF$, as reported in Ref. 21, where the experimental and calculation details are presented and discussed. In other words,

at the end of isothermal crystallization, the analyzed polymers exhibit different three-phase compositions, with decreasing crystal fraction and increasing rigid amorphous content upon increase of the concentration of ethylene co-units. The specific RAF, determined by normalization of the RAF to the crystal fraction, is also affected by the chain composition, due to accumulation of ethylene segments at the basal planes of the crystal lamellae in the copolymers. It provides information about the average thickness of the rigid amorphous layer coupled with the crystals, which increases with ethylene content.²¹

Table 2. Crystal fraction (X_{cry}), mobile amorphous fraction (MAF), rigid amorphous fraction (RAF), and specific RAF (RAF_{sp}) of iPB-1 homopolymer and random butene-1/ethylene copolymers after isothermal crystallization at the indicated temperatures (T_c) for 25 min.²¹

Ethylene (mol%)	T_c (°C)	X_{cry}	MAF	RAF	RAF_{sp}
0	90	0.61	0.20	0.19	0.31
1.5	70	0.41	0.33	0.26	0.63
4.3	40	0.24	0.45	0.31	1.30

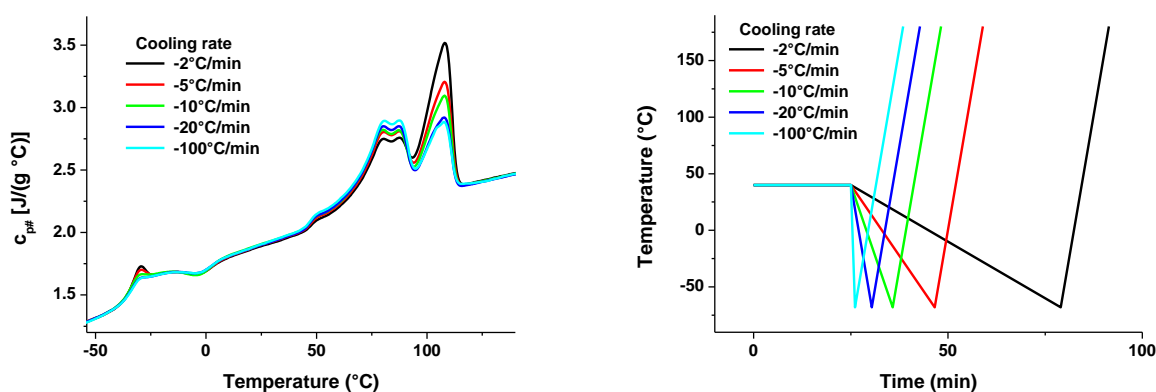


Figure 3. Apparent specific heat capacity ($c_{p\#}$) of the butene-1/ethylene random copolymer containing 4.3 mol% of ethylene, isothermally crystallized at 40 °C for 25 min, cooled to -70 °C at the indicated rates, and then heated at 20 K min⁻¹ (left plot). The temperature-time profile is illustrated on the right.

Cooling to temperatures below T_c and re-heating causes partial transformation of the tetragonal condis crystals to the trigonal structure. The extent of this transformation is affected by the cooling and heating rates. Figure 3 shows the apparent specific heat capacity ($c_{p\#}$) of the random copolymer with 4.3 mol% ethylene, isothermally crystallized at 40 °C for 25 min, cooled to -70 °C

at the indicated rates, and then heated at 20 K min⁻¹ until completion of melting. The effect of variation of the heating rate is presented in Figure 4, which shows the thermal analysis of the same copolymer, isothermally crystallized at 40 °C for 25 min, rapidly cooled to -70°C, and then heated at different rates until completion of melting.

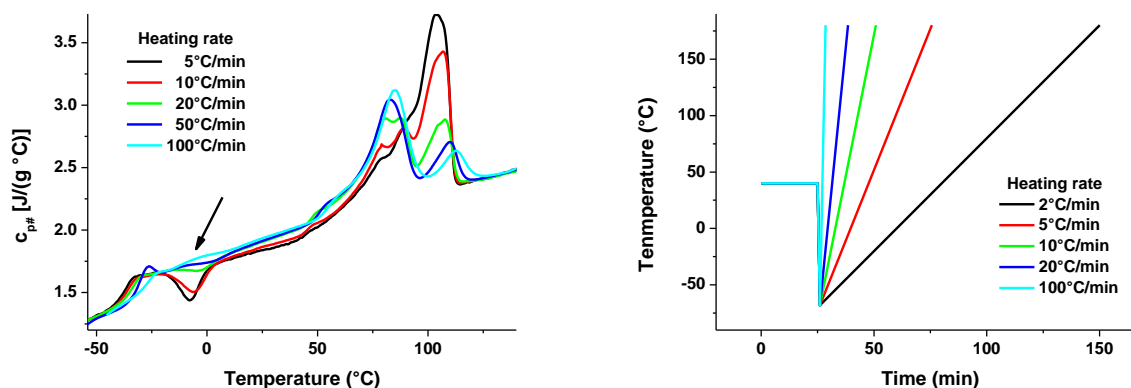


Figure 4. Apparent specific heat capacity ($c_{p\#}$) of the butene-1/ethylene random copolymer containing 4.3 mol% of ethylene, isothermally crystallized at 40 °C for 25 min, cooled to -70 °C at the nominal rate of 100 K min⁻¹, and then heated at the indicated rates (left plot). The temperature-time profile is illustrated on the right.

Figure 3 reveals that upon heating at 20 K min⁻¹, up to about 40 °C, i.e., to T_c , the experimental $c_{p\#}$ curves overlap, with the only exception of a small enthalpy-relaxation peak at the glass transition temperature of the MAF, which originates from the difference between the cooling and heating rates and the residence time of the sample in the glassy state.³⁰ The data shown in Figure 3 display no significant variation of the heat-capacity step at the glass transition of the MAF ($T_{g,MAF}$), which indicates that no additional crystallization, and no additional vitrification of rigid amorphous portions occur during cooling from the crystallization temperature down to below $T_{g,MAF}$. Moreover, the weak exotherm around 0 °C, also seen in Figure 2, is unlikely to be ascribed to cold crystallization, since it is not affected by the prior cooling rate.³¹ Conversely, the rate of cooling the sample from T_c to below $T_{g,MAF}$ largely determines the Form I to Form II ratio: at low cooling rates there is a longer residence time in the temperature range where the transition rate from the tetragonal to the trigonal modification is maximal, which results in a higher Form I crystal content. Major changes of the experimental $c_{p\#}$ profile after isothermal crystallization at $T_c = 40$ °C and cooling to below $T_{g,MAF}$, are observed upon variation of the heating rate, as illustrated in Figure 4. As expected, the glass transition moves to higher temperatures with the heating rate,³⁰ but this does not involve a variation of the heat capacity step at $T_{g,MAF}$, i.e., no variation of the mobile amorphous content and presumably also no variation in both crystal and rigid amorphous fractions.

At completion of the glass transition, a thermal event appears below 0 °C, as evidenced by the arrow in Figure 4, which is strongly affected by the heating rate. It appears as an exotherm, which becomes increasingly less intense at high heating rates. In other words, at low heating rates there is more time for this thermal event to occur in the temperature range from -20 to +10 °C, which results in a larger exotherm at lower heating rates. The heating rate also influences the Form II-Form I transformation, which occurs during the scan at an extent that increases with reducing the heating rate, similarly to the exothermic event below 0 °C, which suggests a correlation between the two processes.

In order to shed light into this thermal event occurring below 0 °C, the iPB-1 homopolymer and the copolymers were isothermally crystallized at T_c for 25 min, then annealed for various times at temperatures ranging from -30 to +30°C, and the relative content of Form II and Form I crystals was analyzed as function of the annealing time and temperature.

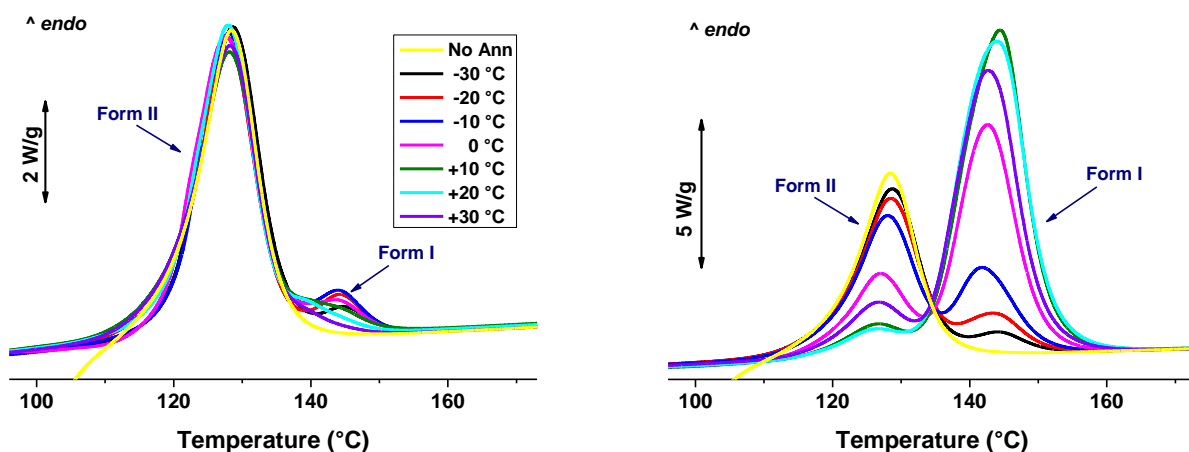


Figure 5. iPB-1 homopolymer, isothermally crystallized at 90°C for 25 min and annealed at the indicated temperatures for 1 h (left plot) or 24 h (right plot), then heated at 100 K min⁻¹. The DSC plot taken immediately after isothermal crystallization at $T_c = 90$ °C (No Ann) is also shown.

The influence of temperature (T_a) on the Form II to Form I transformation is illustrated in Figure 5 for iPB-1, isothermally crystallized at $T_c = 90$ °C, then annealed at various temperatures for two selected times (t_a). Figure 5-a shows the DSC analysis of iPB-1 homopolymer after 60 min of annealing at -30 °C $\leq T_a \leq +30$ °C, that is at the initial stages of the Form II to Form I transformation. This is compared to the same sample not subjected to annealing at low temperatures, but heated immediately after isothermal crystallization at $T_c = 90$ °C. The DSC plot of the non-annealed iPB-1, shown in Figure 5-a, displays a single melting endotherm, centered at 128 °C, which reveals the presence of only Form II mesophase after completion of isothermal crystallization. Annealing at temperatures below T_c for 1 hour results in the appearance of a second

weak endotherm at a higher temperature, around 144 °C, due to melting of Form I crystals, and a slight decrease in the low-temperature peak. Extension of annealing to $t_a = 24$ hours results in considerable variation of the peak areas, as illustrated in Figure 5-b. The DSC plot still displays two melting peaks, but the size of the two endotherms varies with the annealing temperature: a decrease in the endotherm associated to melting of Form II mesophase corresponds to an increase in the area of the melting peak of Form I crystals, but not of an identical quantity, due to the different bulk heat of fusion of the two crystal modifications of iPB-1.¹⁴ In other words, Form II crystals transform to Form I mostly during isothermal annealing at low temperatures, and the extent of the transformation is largely affected by T_a . As shown in Figure 5-b, the Form I to Form II transformation is close to completion after 24 hours at $T_a = +10 \div +20$ °C, whereas lower amounts of Form I seem to be developed after annealing for the same times at lower or higher temperatures. Conversely, at the early stages of the transformation, short-time annealing at $-20 \div -10$ °C leads to development of larger amounts of Form I, compared to annealing at different temperatures, as suggested by the data presented in Figure 5-a.

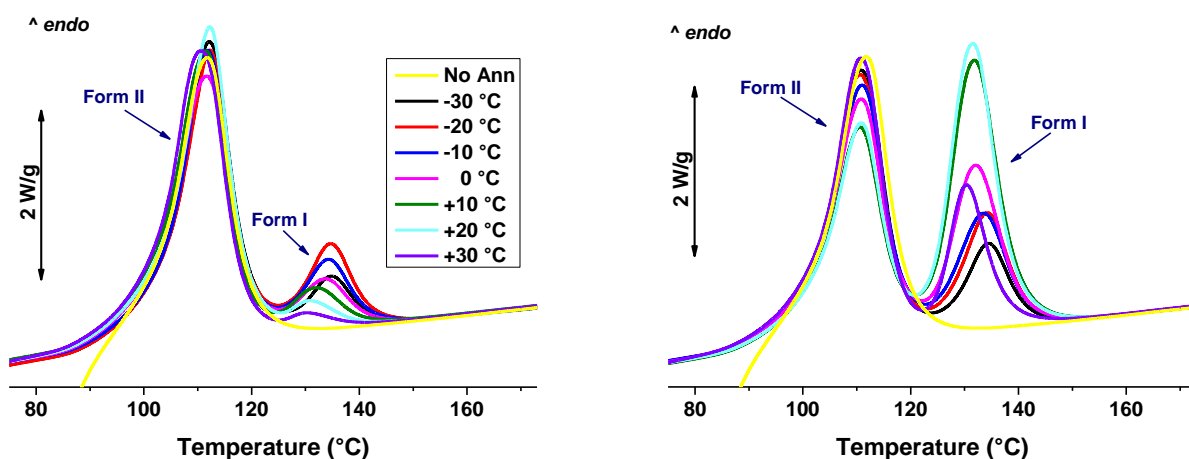


Figure 6. Butene-1/ethylene random copolymer containing 1.5 mol% of ethylene, isothermally crystallized at 70°C for 25 min and annealed at the indicated temperatures for 1 h (left plot) or 8 h (right plot), then heated at 100 K min⁻¹. The DSC plot taken immediately after isothermal crystallization at $T_c = 70$ °C (No Ann) is also shown.

The thermal analysis of the butene-1/ethylene random copolymer containing 1.5 mol% of ethylene segments, after isothermal crystallization at $T_c = 70$ °C for 25 min and annealing at various temperatures, is presented in Figure 6. In the same figure, the DSC plot of the sample not subjected to annealing at low temperatures, and heated immediately after isothermal crystallization is also shown. Figure 6-a discloses the effects of annealing for 1 hour at low temperatures of the random copolymer containing 1.5 mol% of ethylene units. Compared to the iPB-1 homopolymer, larger

amounts of Form I develop from the original Form II crystals, at parity of annealing time t_a , in agreement with literature data, which indicate that random copolymerization of butene-1 with short-chain olefins, like ethylene or propylene, accelerates the Form II to I transformation rate.^{3,11,17,19,22} As shown also for the iPB-1 homopolymer in Figure 5-a, after short-time annealing ($t_a = 1$ hour), larger amounts of Form I crystals originate from Form II mesophase upon annealing at $T_a = -20^\circ\text{C}$, whereas annealing at lower or higher temperatures leads to a lower degree of conversion (Figure 6-a). The effect of annealing the random copolymer containing 1.5 mol% of ethylene for 8 hours at various temperatures is illustrated in Figure 6-b. When the semicrystalline copolymer is maintained for 8 hours at low temperatures, considerable Form II to Form I transformation occurs, as probed by the large endotherms centered at 131°C , due to melting of trigonal Form I crystals, and the corresponding reduced peak at 111°C , due to melting of the tetragonal Form II modification. After 8 hours of permanence at the various T_a 's, the transformation occurs to a larger extent upon annealing at $T_a = +10 \div +20^\circ\text{C}$, as indicated by the more intense high-temperature endotherm, and the corresponding reduced low-temperature melting peaks (Figure 6-b).

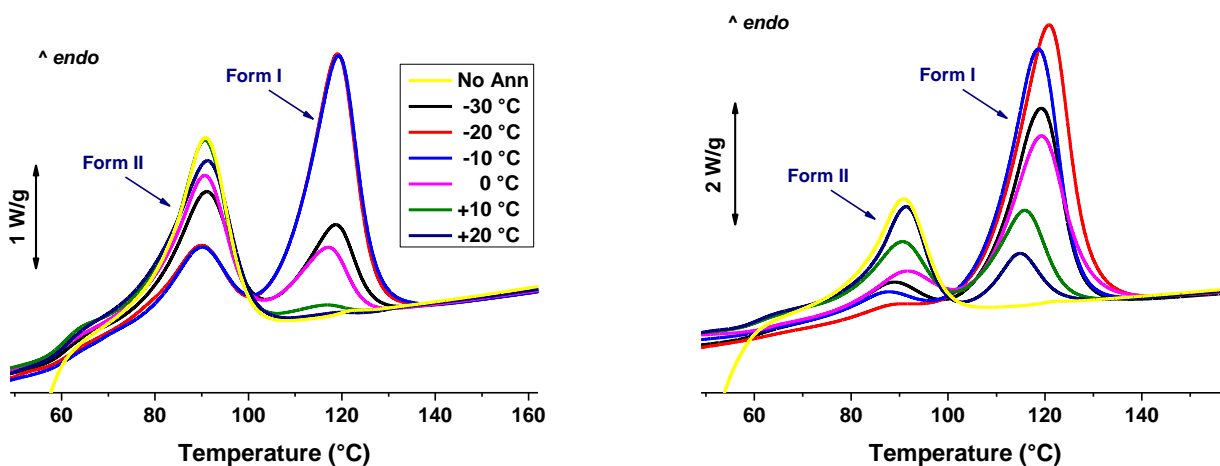


Figure 7. Butene-1 / ethylene random copolymer containing 4.3 mol% of ethylene, isothermally crystallized at 40°C for 25 min and annealed at the indicated temperatures for 10 min (left plot) or 4 h (right plot), then heated at 100 K min^{-1} . The DSC plot taken immediately after isothermal crystallization at $T_c = 40^\circ\text{C}$ (No Ann) is also shown.

Figure 7 illustrates the effect of temperature on the Form II to Form I transformation in the random copolymer containing 4.3 mol% of ethylene, which was isothermally crystallized at $T_c = 40^\circ\text{C}$ for 25 min before the low temperature annealing. Data are compared with the thermal profile of the same polymer heated immediately after isothermal crystallization at $T_c = 40^\circ\text{C}$. The latter plot reveals that even at the end of isothermal crystallization, some small amounts of Form I crystals have already converted from Form II, due to the low crystallization temperature, as well as to the

fast solid-solid transformation kinetics of this grade. Direct formation of Form I from the melt, leading to Form I' crystals, was proven in poly(butene-1) grades with low isotacticity, but their melting point is much lower than that of Form I crystals.^{23,25,32-34} The DSC plot of the as-crystallized sample, shown in Figure 7, indicate that melting of Form I crystals occurs around 125 °C, which is typical of Form I developed from transformation of Form II mesophase, not directly grown from the melt. Annealing the copolymer at temperatures between -30 and +20 °C for a time as short as $t_a = 10$ min leads to sizeable transformation of Form II mesophase to Form I crystals, as shown in Figure 7-a. The transformation occurs to a larger extent at $T_a = -20 \div -10$ °C, whereas a lower degree of transformation is observed upon annealing at lower or higher temperatures. Annealing the copolymer at the same temperatures for a much longer time ($t_a = 4$ h) leads to a higher degree of Form II to Form I transformation, which is close to completion at $T_a = -20$ °C, and proceeds with a slower kinetics at higher or lower temperatures, as seen in Figure 7-b.

The effect of variation of annealing temperatures and times on the transformation kinetics was quantified by integration of the two endotherms in Figures 5-7, using the multiple peakfit procedure detailed in the Experimental Part. This allowed to determine the degree of Form II to Form I conversion, which is presented in Figures 8-10 as $X_{\text{cry}}(\text{I}) / X_{\text{cry}}(\text{Tot})$ for the three analyzed compositions.

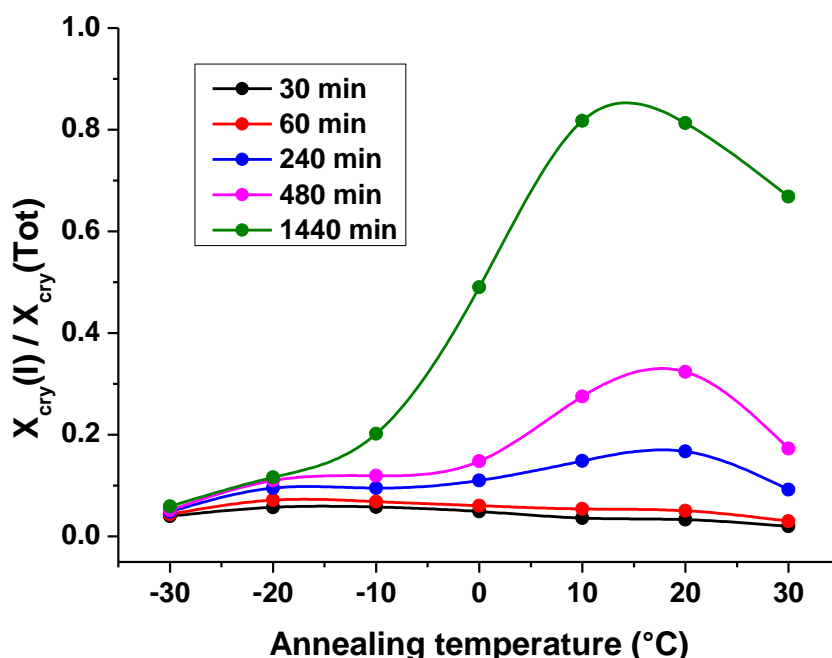


Figure 8. Ratio between crystal fraction of Form I $X_{\text{cry}}(\text{I})$ to total crystal fraction $X_{\text{cry}}(\text{Tot})$, of iPB-1 homopolymer as function of the annealing temperature at the indicated times.

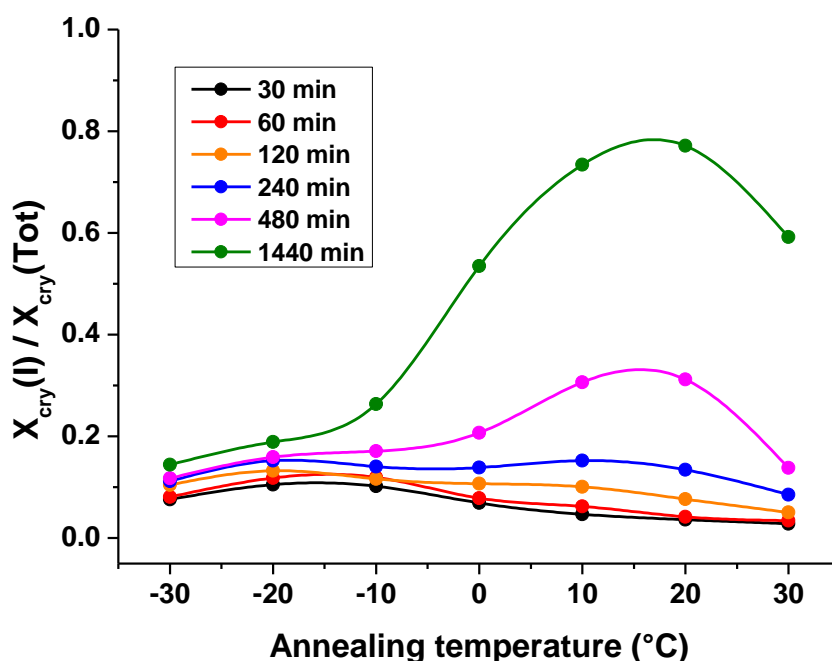


Figure 9. Ratio between crystal fraction of Form I $X_{\text{cry}}(\text{I})$ to total crystal fraction $X_{\text{cry}}(\text{Tot})$, of butene-1/ethylene random copolymer containing 1.5 mol % of ethylene, as function of the annealing temperature at the indicated times.

As illustrated in Figure 8 for the iPB-1 homopolymer, the maximum transformation rate is observed around $T_a = +20$ °C, in agreement with literature data.^{1,12-14} At the initial stages of the conversion, at $X_{\text{cry}}(\text{I}) / X_{\text{cry}}(\text{Tot}) < 0.15$, a weak maximum also appears at -20 °C, as already observed in Figure 5-a, suggesting that a faster kinetics is observed around -20 °C at the beginning of the solid-solid transformation. The presence of 1.5 mol% of ethylene units results in a lightly varied solid-solid transformation kinetics upon annealing, as illustrated in Figure 9. The Form II to Form I transformation rate appears slightly faster than in iPB-1 homopolymer at low degree of conversion. Similar to the data shown in Figure 8, and as also shown in Figure 6-a, a weak maximum in the transformation rate appears around -20 °C, at $X_{\text{cry}}(\text{I}) / X_{\text{cry}}(\text{Tot}) < 0.2$, together with a more pronounced maximum when the solid-solid transformation approaches completion, around +20 °C.

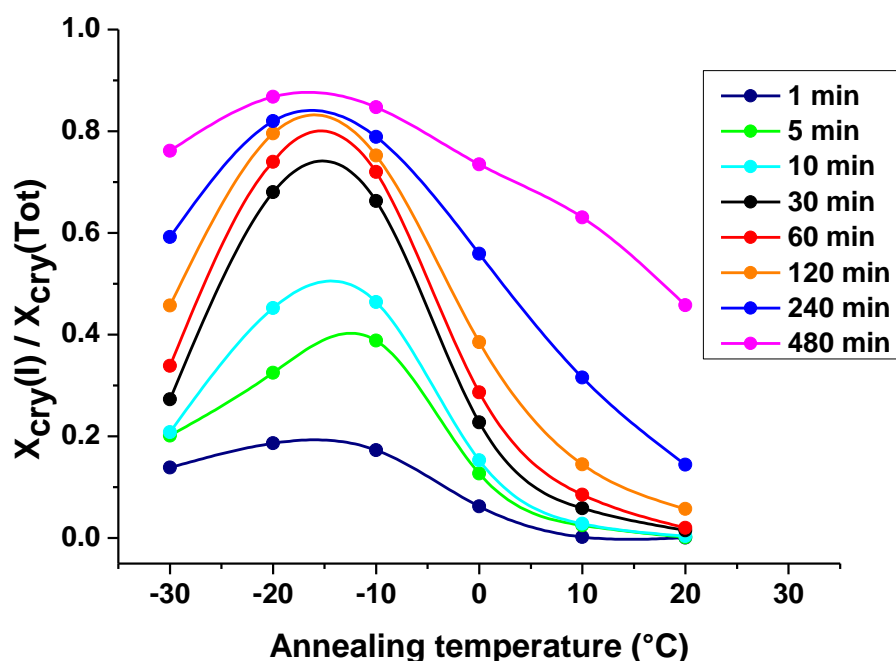


Figure 10. Ratio between crystal fraction of Form I $X_{\text{cry(I)}}$ to total crystal fraction $X_{\text{cry(Tot)}}$, of butene-1/ethylene random copolymer containing 4.3 mol % of ethylene, as function of the annealing temperature at the indicated times.

The transition kinetics becomes much faster when larger amounts of ethylene units are copolymerized with butene-1, as shown by the data presented in Figure 10, where the degree of Form II to Form I conversion of the copolymer containing 4.3 mol% of ethylene is reported as function of the annealing temperature. The solid-solid transformation approaches completion at much shorter times, compared to the two other analyzed compositions, and the transformation rate appears to have a single maximum at low temperatures, around $-20 \div -10$ °C.

The above results indicate not only that annealing at temperatures between -30 and $+30$ °C leads to sizeable Form II to Form I solid-solid transformation, in agreement with literature data,^{3,22} but also suggest that, at the initial stages of the transition, isothermal annealing at temperatures around $-10 \div -20$ °C leads to a larger degree of transformation than isothermal annealing at higher or lower temperatures. The tetragonal to trigonal crystal transformation occurs not only upon isothermal annealing, but also during heating or cooling, as probed by the data shown in Figures 2-4. The weak exotherm observed in Figures 2-4 in the temperature range $-20 \div +10$ °C, is caused by the solid-solid transformation occurring during heating, which, at the rate of 5 K min^{-1} , for instance, corresponds to a permanence of about 12 min in the temperature range $-30 \div +30$ °C. At higher heating rates, the residence time is lower, which explains the temperature-dependence of the

exotherm below 0 °C, in the low temperature side of the transformation range (see Figures 2-4 and 8-10).

The results reported in Figures 8-10 indicate that the presence of ethylene co-units included in linear butene-1 chains not only accelerates the transformation rate from the Form II mesophase to the stable Form I crystals,^{11,17,22} but also induces a variation in the temperature-dependence of the transformation rate. The low-temperature maximum for Form II to form I transition is also evidenced by the data shown in Figures 5-a, 6-a, 7-a: for short annealing times, a larger Form I develops upon annealing at temperatures around -20 ÷ -10 °C. These data are highly reproducible, as a faster transition kinetics at short annealing time has been observed upon annealing at such low temperatures for all the analyzed samples. Discussion of the effect of ethylene chain segments should take into account the mechanism of this polymorphic transformation, which is still under discussion, despite its extensive investigation since 1964.^{1,13,35,36} The solid-solid transition most probably occurs *via* nucleation and growth³⁷⁻³⁸ and different mechanisms have been proposed,¹⁶ but the exact nature of the processes that initiate the transitions, and their molecular translation in terms of transition kinetics have not been determined yet.³⁹⁻⁴¹ However, all the proposed mechanisms hypothesize a two-step process, involving nucleation and growth. This may be correlated with the two maxima in the degree of transformation, reported in Figures 8-10 for both iPB-1 homopolymer and the random butene-1/ethylene copolymers: a first one at low degrees of conversion, which may be linked to a faster nucleation stage at low temperatures, around -20 °C, and one at higher temperatures around +20 °C, related to the growth process at higher degrees of conversion.

To rationalize the effect of copolymerization with ethylene on the kinetics of Form II to Form I transformation, it should also be considered that in random butene-1/ethylene copolymers the ethylene units are mostly excluded from the crystals and accumulate at the basal planes of the crystal lamellae. Only minor amounts of ethylene co-units are incorporated into Form II mesophase, and migrate into amorphous areas upon transformation to the trigonal stable crystals, as recently demonstrated.^{3,17,20} If the few ethylene segments included within the Form II mesophase act as crystal defects able to nucleate the solid-solid transformation, their contribution appears too low to determine the remarkable composition-dependence of the Form II to Form I transformation rate shown in Figures 5-10. The experimental data reveal not only that the transformation rate varies with copolymer composition, but also that the presence of ethylene co-units affects the temperature of maximum transformation rate. The latter is determined by a balance between chain mobility and driving force for the transformation.²² It can be assumed that the chain mobility within the crystals does not significantly vary with copolymer composition, since ethylene co-units are mostly excluded from the crystals. Conversely, it is likely that the mobility of the chain segments at the

amorphous/crystal interface is highly affected by the presence of ethylene co-units. A varied chain mobility was proven to affect the Form II to Form I transformation rate also in stereodeficient isotactic poly(butene-1), since *rr* triads, as chain defects, increase the flexibility of iPB-1 chains, similarly to copolymerization with ethylene.^{23,33,42} Moreover, copolymerization of butene-1 with ethylene induces significant variation in the fold-surface composition, as the ethylene co-units accumulate at the crystal basal planes. This leads to a distinct increase in the rigid amorphous fraction (RAF) with increasing concentration of ethylene co-units.²¹ The RAF is a measure of the number of molecule segments traversing the crystalline-amorphous interface, that is, of the degree of covalent coupling of crystals and amorphous phase. The specific RAF, determined by normalization of the RAF to the crystal fraction, amounts to 30% in iPB-1 homopolymer, and increases to more than 100% in the copolymers with 4.3 mol% of ethylene co-units, as reported in Table 2. In the random butene-1/ethylene copolymers, the lamellar thickness is not affected by the copolymer composition, but only by crystallization temperature, as quantified in Ref. 43-44. Independently of the crystallization temperature, a higher specific RAF means that either the ratio between the RAF layer at the top and bottom fold-surfaces and the lamellar thickness is higher or, if the lamellar thickness is lower, that the lamellar surfaces and, as a consequence, the RAF layer is larger. The immobilized amorphous layers include, besides iPB-1 segments, also composition-dependent amounts of ethylene units, which are confined to the crystal-amorphous boundary upon crystal growth.²⁰⁻²¹ This leads to a marked increase in the free energy of the crystal-fold surface due to copolymerization.²⁰

In the iPB-1 homopolymer, the RAF coupled with the Form II mesophase completely devitrifies around 50 °C, whereas when the RAF is coupled with Form I lamellae, it completes its glass transition only at about 100 °C.^{15,45} In other words, at the temperature of maximum Form II to Form I transformation rate (+20 °C), in iPB-1 the RAF is partially mobilized, and only 10-15% of the RAF is still vitrified.^{15,46} At the amorphous/crystal interface of the butene-1/ethylene copolymers, the RAF is made of both butene-1 and ethylene chain segments. Mobilization of the ethylene segments can occur at a temperature much lower than that of the amorphous iPB-1 segments,⁴⁶ hence it is likely that the varied chain composition affects the mobility of the rigid amorphous portions, which in the copolymers can become fully mobilized at much lower temperatures. The varied mobility of the amorphous chains coupled with the crystals affects the local stress transmitted to the crystals, and may facilitate the solid-solid transformation. This may cause a shift of the maximum transition rate to lower temperatures, probed by the data presented in Figure 10. In other words, the temperature-dependence of the maximum Form II to Form I transformation rate, linked to the varied composition of the rigid amorphous portion at the lamellar

basal planes of the crystals, suggests the hypothesis of a connection between interfaces and crystal lamellae rearrangements, which in iPB-1-based copolymers can produce an acceleration in the solid-solid transformation from the condic mesophase to the trigonal crystals.³⁶ A similar influence of the rigid amorphous fraction on the crystal rearrangements that lead to multiple melting behavior has been recently proven for a number of semicrystalline polymers, including poly(ethylene terephthalate),^{47,48} *cis*-1,4-polybutadiene,⁴⁹ isotactic polystyrene,⁵⁰ and poly[(R)-3-hydroxybutyrate].⁵¹

Conclusions

The point-by point analysis of the kinetics of the solid-solid transformation from the tetragonal Form II condic modification to the trigonal Form I crystals in isotactic poly(butene-1) and its random copolymers with ethylene, detailed in this contribution, allowed to identify, for the first time, the occurrence of two maxima in the rate of transformation vs. annealing temperature. All the previous reports indicate a single maximum rate, around room temperature, whereas the data illustrated and discussed in this manuscript evidence the occurrence of a weaker maximum also at lower temperatures, around -20 °C. The low-temperature maximum becomes even more evident in the analyzed ethylene/butene-1 random copolymers, which also display a dual transformation kinetics. The available literature studies on the irreversible tetragonal to trigonal crystals transformation in isotactic poly(butene-1) propose a two step mechanism, made of nucleation and growth, which seems to be supported by the data reported here.

Copolymerization with ethylene results not only in a sizably faster kinetics of the polymorphic transformation, but also affects the maximum transformation rate. In the ethylene/butene-1 random copolymers, not only the transformation rate becomes faster, but there is also a shift to lower temperatures of the maximum transformation rate. This observation has been linked to the varied composition of the amorphous layers coupled with the crystals, which becomes increasingly more mobile and thicker with the increase of ethylene co-units in the copolymers. This confirms the role played by rigid amorphous segments coupled with the crystals in reorganization of the crystal phase into more stable structures, which, to date, has been probed by analysis of multiple melting behavior in a number of semicrystalline polymers.

Acknowledgments

RA acknowledges financial support by the Deutsche Forschungsgemeinschaft (DFG) (Grant AN 212/12). MLDL wishes to thank Dr. Barbara Coppola (Napoli, Italy) for useful discussions.

References

1. Rubin I. D. *Poly(1-Butene): Its Preparation and Stability*; Gordon and Breach Science Publishers Inc.: New York, 1968.
2. Petraccone, V.; Pirozzi, B.; Frasci, A.; Corradini, P. Polymorphism of Isotactic Poly- α -Butene: Conformational Analysis of the Chain and Crystalline Structure of Form 2. *Eur. Polym. J.* **1976**, *12*, 323-327.
3. Turner-Jones, A. Cocrystallization in Copolymers of α -Olefins II—Butene-1 Copolymers and Polybutene Type II/I Crystal Phase Transition. *Polymer* **1966**, *7*, 23-59.
4. Wunderlich, B.; Grebowicz, J. Thermotropic Mesophases and Mesophase Transitions of Linear, Flexible Macromolecules. *Adv. Polym. Sci.* **1984**, *60*, 1–59.
5. Maring, D.; Meurer, B.; Weill, G. ^1H NMR Studies of Molecular Relaxations of Poly-1-Butene. *J. Polym. Sci. Part B: Polym. Phys.* **1995**, *33*, 1235-1247.
6. Maring, D.; Wilhelm, M.; Spiess, H. W.; Meurer, B.; Weill, G. Dynamics in the Crystalline Polymorphic Forms I and II and Form III of Isotactic Poly-1-Butene. *J. Polym. Sci. Part B: Polym. Phys.* **2000**, *38*, 2611-2624.
7. Natta, G.; Corradini, P.; Bassi, I. W. Crystal Structure of Isotactic Poly- α -Butene. *Nuovo Cimento* **1960**, *15*, 52-67.
8. Armeniades, C. D.; Baer, E. Effect of Pressure on the Polymorphism of Melt Crystallized Polybutene-1. *J. Macromol. Sci. Phys.* **1967**, *1*, 309-334.
9. Chau, K. W.; Geil, P. H. Solution History Effects in Polybutene-1. *J. Macromol. Sci. Phys.* **1984**, *23*, 115-142.
10. Yamashita, M.; Hoshino, A.; Kato, M. Isotactic Poly(Butene-1) Trigonal Crystal Growth in the Melt. *J. Polym. Sci. Part B: Polym Phys.* **2007**, *45*, 684-697.
11. Azzurri, F.; Gómez, M. A.; Alfonso, G. C.; Ellis, G.; Marco, C. Time-Resolved SAXS/WAXS Studies of the Polymorphic Transformation of 1-Butene/Ethylene Copolymers. *J. Macromol. Sci., Part B – Phys.* **2004**, *B43*, 177-189.
12. Azzurri, F.; Flores, A.; Alfonso, G. C.; Baltá Calleja, F. J. Polymorphism of Isotactic Poly(1-butene) as Revealed by Microindentation Hardness. 1. Kinetics of the Transformation. *Macromolecules* **2002**, *35*, 9069-9073.
13. Silvestre, C.; Di Lorenzo, M. L.; Di Pace, E. Crystallization of Polyolefins In Handbook of Polyolefins; Vasile C., Ed.; Marcel Dekker, Inc.: New York, 2000, Chapter 9, pp.223-248.
14. Alfonso, G. C.; Azzurri, F.; Castellano, M. Analysis of Calorimetric Curves Detected During the Polymorphic Transformation of Isotactic Polybutene-1. *J. Therm. Anal. Calorim.* **2001**, *66*, 197-207.

15. M. L. Di Lorenzo, M. C. Righetti, B. Wunderlich, Influence of Crystal Polymorphism on the Three-Phase Structure and on the Thermal Properties of Isotactic Poly(1-butene). *Macromolecules* **2009**, *42*, 9312–9320.
16. Cocca, M.; Androsch, R.; Righetti, M. C.; Malinconico, M.; Di Lorenzo, M. L. Conformationally Disordered Crystals and their Influence on Material Properties: The Cases of Isotactic Polypropylene, Isotactic Poly(1-Butene), and Poly(L-Lactic Acid). *J. Mol. Struct.* **2014**, *1078*, 114–132
17. Stolte, I.; Androsch, R. Kinetics of the Melt – Form II Phase Transition in Isotactic Random Butene-1/Ethylene Copolymers. *Polymer* **2013**, *54*, 7033-7040.
18. Stolte, I.; Androsch, R. Comparative Study of the Kinetics of Non-Isothermal Melt Solidification of Random Copolymers of Butene-1 with Either Ethylene or Propylene. *Coll. Polym. Sci.* **2014**, *292*, 1639–1647.
19. Gianotti, G.; Capizzi, A. Butene-1/Propylene Copolymers, Influence of the Comonomeric Units on Polymorphism. *Makromol. Chem.* **1969**, *124*, 152-159.
20. Stolte, I. Di Lorenzo, M. L.; Androsch, R. Spherulite Growth Rate and Fold Surface Free Energy of the Form II Mesophase in Isotactic Polybutene-1 and Random Butene-1/Ethylene Copolymers. *Coll. Polym. Sci.* **2014**, *292*, 1479–1485.
21. Di Lorenzo, M. L.; Androsch, R.; Stolte, I. Tailoring the Rigid Amorphous Fraction of Isotactic Polybutene-1 by Ethylene Chain Defects. *Polymer* **2014**, *55*, 6132-6139.
22. Azzurri, F.; Alfonso, G. C.; Gomez, M. A.; Marti, M. C.; Ellis, G.; Marco, C. Polymorphic Transformation in Isotactic 1-Butene/Ethylene Copolymers. *Macromolecules* **2004**, *37*, 3755-3762.
23. De Rosa, C.; Auriemma, F.; Resconi, L. Metalloorganic Polymerization Catalysis as a Tool to Probe Crystallization Properties of Polymers: The Case of Isotactic Poly(1-Butene). *Angew. Chem.* **2009**, *121*, 10055-10058.
24. Yamashita, M. Direct Crystal Growth of Isotactic Polybutene-1 Trigonal Phase in the Melt: In-Situ Observation. *J. Cryst. Growth* **2007**, *210*, 1739-1743.
25. Yamashita, M. Melt Growth Rate and Growth Shape of Isotactic Polybutene-1 Tetragonal Crystals. *J. Cryst. Growth* **2009**, *311*, 556-559.
26. Yamashita, M. Crystal Growth Kinetics and Morphology of Isotactic Polybutene-1 Trigonal Phase in the Melt. *J. Cryst. Growth* **2009**, *311*, 560-563.
27. Nase, M.; Androsch, R.; Langer, B.; Baumann, H. J.; Grellmann, W. Effect of Polymorphism of Isotactic Polybutene-1 on Peel Behavior of Polyethylene/Polybutene-1 Peel Systems. *J. Appl. Polym. Sci.* **2008**, *107*, 3111-3118.

28. Nase, M.; Funari, S. S.; Michler, G. H.; Langer, B. Grellmann, W.; Androsch, R. Structure of Blown Films of Polyethylene/Polybutene-1 Blends. *Polym. Eng. Sci.* **2010**, *50*, 249-256.
29. Product information, Lyondell Basell, <https://polymers.lyondellbasell.com/portal/site/basell/polybutene-1>.
30. Wunderlich, B. *Thermal Analysis of Polymeric Materials*; Springer, 2005.
31. Androsch, R.; Di Lorenzo, M.L. Kinetics of Crystal Nucleation of Poly(L-lactic acid). *Polymer* **2013**, *54*, 6882-6885.
32. Jr Boor, J.; Youngman, E. A. Polymorphism in Poly-1-Butene: Apparent Direct Formation of Modification I. *J. Polym. Sci. B* **1964**, *2*, 903-907.
33. De Rosa, C.; Auriemma, F.; Ruiz de Ballesteros, O.; Esposito, G.; Laguzza, D.; Di Girolamo, R.; Resconi, L. Crystallization Properties and Polymorphic Behavior of Isotactic Poly(1-Butene) from Metallocene Catalysts: The Crystallization of Form I from the Melt. *Macromolecules* **2009**, *42*, 8286-8297.
34. Stolte, I.; Fischer, M.; Roth, R.; Borreck, S.; Androsch, R. Morphology of Form I' crystals of polybutene-1 formed on melt-crystallization. *Polymer* **2015**, in press, [doi:10.1016/j.polymer.2015.02.034](https://doi.org/10.1016/j.polymer.2015.02.034).
35. Holland, V. F.; Miller, R. L. Isotactic Polybutene-1 Single Crystals: Morphology. *J. Appl. Phys.* **1964**, *35*, 3241-3248.
36. Samon, J. M.; Schultz, J. M.; Hsiao, B. S.; Wu, J.; Khot, S. Structure Development During Melt Spinning and Subsequent Annealing of Polybutene-1 Fibers. *J. Polym. Sci., Part B: Polym. Phys.* **2000**, *38*, 1872-1882.
37. Gohil, R. M.; Miles, M. J.; Petermann, J. On the Molecular Mechanism of the Crystal Transformation (Tetragonal-Hexagonal) in Polybutene-1. *J. Macromol. Sci.* **1982**, *B 21*, 189-201.
38. Fujiwara, Y. II-I Phase Transformation of Melt-Crystallized Oriented Lamellae of Polybutene-1 by Shear Deformation. *Polym. Bull.* **1985**, *13*, 253-258.
39. Kopp, S.; Wittmann, J. C.; Lotz, B. Phase II to Phase I Crystal Transformation in Polybutene-1 Single Crystals: A Reinvestigation. *J. Mater. Sci.* **1994**, *29*, 6159-6166.
40. Tosaka, M.; Kamijo, T.; Tsuji, M.; Kohjiya, S.; Ogawa, T.; Isoda, S.; Kobayashi, T. High-Resolution Transmission Electron Microscopy of Crystal Transformation in Solution-Grown Lamellae of Isotactic Polybutene-1. *Macromolecules* **2000**, *33*, 9666-9672.
41. Marigo, A.; Marega, C.; Cecchin, G.; Collina, G.; Ferrara, G. Phase Transition II → I in Isotactic Poly-1-Butene: Wide- and Small-Angle X-Ray Scattering Measurements. *Eur. Polym. J.* **2000**, *36*, 131-136.

42. De Rosa, C.; Ruiz de Ballesteros, O.; Auriemma, F.; Di Girolamo, R.; Scarica, C.; Giusto, G.; Esposito, S.; Guidotti, S.; Camurati, I. Polymorphic Behavior and Mechanical Properties of Isotactic 1-Butene–Ethylene Copolymers from Metallocene Catalysts. *Macromolecules* **2014**, *47*, 4317–4329.
43. Wang, Y.; Lu, Y.; Jiang, Z.; Men, Y. Molecular Weight Dependency of Crystallization Line, Recrystallization Line, and Melting Line of Polybutene-1. *Macromolecules* **2014**, *47*, 6401–6407.
44. Wang, Y.; Lu, Y.; Zhao, J.; Zhiyong, J.; Men, Y. Direct Formation of Different Crystalline Forms in Butene-1/Ethylene Copolymer via Manipulating Melt Temperature. *Macromolecules* **2014**, *47*, 8653–8662.
45. Di Lorenzo, M. L.; Righetti, M. C. The Three-Phase Structure of Isotactic Poly(1-Butene). *Polymer* **2008**, *49*, 1323–1331.
46. Wunderlich, B. Reversible Crystallization and the Rigid–Amorphous Phase in Semicrystalline Macromolecules. *Prog. Polym. Sci.* **2003**, *28*, 383–450.
47. Di Lorenzo, M. L.; Righetti, M. C.; Cocca, M.; Wunderlich, B. Coupling between Crystal Melting and Rigid Amorphous Fraction Mobilization in Poly(ethylene terephthalate). *Macromolecules* **2010**, *43*, 7689–7694.
48. Righetti, M. C.; Laus, M.; Di Lorenzo, M. L. Rigid Amorphous Fraction and Melting Behavior of Poly(Ethylene Terephthalate). *Coll. Polym. Sci.* **2014**, *292*, 1365–1374.
49. Di Lorenzo, M. L. The Melting Process and the Rigid Amorphous Fraction of *cis*-1,4-Polybutadiene. *Polymer* **2009**, *50*, 578–584.
50. Righetti, M. C.; Tombari, E.; Di Lorenzo, M. L. Crystalline, Mobile Amorphous and Rigid Amorphous Fractions in Isotactic Polystyrene. *Eur. Polym. J.* **2008**, *44*, 2659–2667.
51. Righetti, M. C.; Tombari, E.; Di Lorenzo, M. L. The Role of the Crystallization Temperature on the Nanophase Structure Evolution of Poly[(R)-3-Hydroxybutyrate]. *J. Phys. Chem. B* **2013**, *117*, 12303–12311.